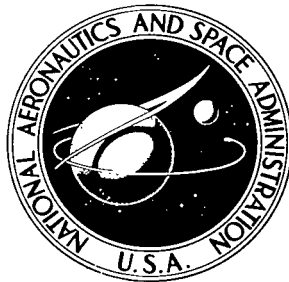


NASA TECHNICAL NOTE



NASA TN D-5324

C. 1

NASA TN D-5324



LOAN COPY: RETURN TO
AFWL (WLIL-2)
KIRTLAND AFB, N MEX

DESIGN OF INJECTORS AND
ABLATIVE THRUST CHAMBERS FOR
A FLOX-PROPANE ROCKET ENGINE
WITH A 1.2-INCH THROAT DIAMETER

by Jerry M. Winter, Donald A. Peterson, and Albert J. Pavli

*Lewis Research Center
Cleveland, Ohio*

NATIONAL AERONAUTICS AND SPACE ADMINISTRATION • WASHINGTON, D. C. • JULY 1969



0132321

DESIGN OF INJECTORS AND ABLATIVE THRUST CHAMBERS
FOR A FLOX-PROPANE ROCKET ENGINE WITH A
1.2-INCH THROAT DIAMETER

By Jerry M. Winter, Donald A. Peterson, and Albert J. Pavli

Lewis Research Center
Cleveland, Ohio

NATIONAL AERONAUTICS AND SPACE ADMINISTRATION

For sale by the Clearinghouse for Federal Scientific and Technical Information
Springfield, Virginia 22151 - CFSTI price \$3.00

ABSTRACT

An in-house study was conducted for the design and testing of liquid FLOX-propane 1.2-inch- (3.05-cm-) throat-diameter rocket engines. Experimental characteristic velocity efficiency as a function of oxidant-to-fuel ratio was determined for four different injector types. An erosion-free 300-second continuous firing capability was demonstrated using a graphite cloth - phenolic chamber and nozzle operating at 100-psia (689-kN/m²) chamber pressure and at an oxidant-to-fuel ratio of 4.5 with a delivered characteristic velocity efficiency level of 95.4 percent (97.5 percent corrected). Erosion-free operation at 200-psia (1378 kN/m²) chamber pressure required use of a graphite throat insert.

CONTENTS

	Page
SUMMARY	1
INTRODUCTION	2
APPARATUS	3
Engine Design	3
Injectors	3
Water-cooled chambers	9
Water-cooled chamber-nozzle combinations	9
Ablative chamber-nozzle combinations	9
Ablative chamber-nozzle with throat insert	11
Facility	12
Test cell	12
Instrumentation	14
Data recording and processing	14
PROCEDURE	15
Engine Assembly	15
Test Procedure	16
RESULTS AND DISCUSSION	16
Injector Evaluation	16
Water-Cooled Chamber and Nozzle Evaluation	22
Ablative Material Evaluation	22
Ablative material performance	22
Effect of chamber pressure on material performance	24
Effect of oxidant-to-fuel ratio on material performance	26
Throat insert testing	29
Vacuum specific impulse	30
SUMMARY OF RESULTS	30
APPENDIX - SYMBOLS	32
REFERENCES	34

DESIGN OF INJECTORS AND ABLATIVE THRUST CHAMBERS
FOR A FLOX-PROPANE ROCKET ENGINE WITH A
1.2-INCH THROAT DIAMETER

by Jerry M. Winter, Donald A. Peterson, and Albert J. Pavli

Lewis Research Center

SUMMARY

Six injectors and three chamber configurations were designed and test fired as components of a FLOX-propane rocket engine. The basic design parameters were explored at a 1.2-inch (3.05-cm) throat diameter with water-cooled and ablative thrust chambers. The range of engine operating conditions included chamber pressures from 100 to 200 psia (689 to 1378 kN/m²) and oxidant-to-fuel ratios (O/F) from 3.5 to 5.0. An oxidant-fuel-oxidant triplet injector with the elements mutually perpendicular gave the highest performance with stable combustion. The characteristic exhaust velocity efficiency was 95.4 percent (97.5 percent corrected) at the design point of 100-psia (689-kN/m²) chamber pressure and an O/F of 4.5. The maximum theoretical equilibrium specific impulse for an expansion area ratio of 40 is at O/F = 4.5. At 100-psia (689-kN/m²) chamber pressure and an O/F of 4.5, a graphite cloth - phenolic ablative chamber-nozzle provided erosion-free operation during a 300-second continuous firing.

Chamber pressure variation gave ηC^* of 97.2 percent (99.3 percent corrected) at 200-psia (1378-kN/m²) chamber pressure and an O/F of 4.5. At 200-psia (1378-kN/m²) chamber pressure, decreasing the O/F from 4.5 to 3.5 significantly decreased the overall erosion rate for a graphite cloth - phenolic chamber nozzle.

An ATJ graphite throat insert tested at 200-psia (1378-kN/m²) chamber pressure and an O/F of 3.5, provided erosion-free operation for approximately 200 seconds and was limited only by ablative charthrough.

Operation of the oxidant-fuel-oxidant triplet injector at 100-psia (689-kN/m²) chamber pressure and an O/F of 3.5 provided a delivered impulse gain of 6 seconds compared to operation at an O/F of 4.5. Since both ablative and combustion performance are enhanced, design of FLOX - liquid-petroleum-gas (LPG) engines for operation significantly below the theoretical maximum impulse O/F should be considered.

INTRODUCTION

Future space missions require propulsion capability for heavier payloads, higher velocities, and greater mission flexibility. Fluorinated oxidizers with liquified petroleum gas fuels provide significant advantages in this regard. A mixture of liquid fluorine and liquid oxygen (FLOX) as the oxidizer used with liquified petroleum gases (LPG) as fuel gives high specific impulse, high bulk density, and hypergolic ignition. The specific impulse of fluorine-oxygen mixtures with hydrocarbons is higher than the impulse with either fluorine or oxygen as the oxidizer alone. The high bulk density of FLOX is due to the high proportion of fluorine (76 percent for maximum impulse when used with propane fuel). With FLOX concentrations of 76-percent fluorine, the oxidant-to-fuel mixture ratio required for theoretical maximum impulse is 4.5 to 1 for propane. This high mixture ratio then permits smaller fuel tanks. The resulting high propellant bulk density also allows greater design flexibility to reentry and landing vehicles because the center of gravity can be more favorably located. Also, FLOX has the advantage of being hypergolic with most LPG fuels when used in the above high fluorine concentrations, thus eliminating the need for ignition systems.

The final choice of a particular LPG to be used as the fuel depends on mission requirements. From an impulse consideration, methane would be superior to all other liquid petroleum gases. As mission duration increases, however, the lower bulk density and lower boiling point of methane must be considered. For certain missions, propane becomes attractive because of its higher bulk density. Propane also has a wider liquid range than methane and is closer to FLOX liquid temperatures than methane. Although not yet determined, the space ignition characteristics of propane should also be better than those of methane because of the lower triple-point pressure of propane. The use of propane will also give a heat-flux reduction because of the higher carbon-to-hydrogen ratio (ref. 1). For these reasons, propane was selected as the fuel for this investigation.

As mentioned before, a unique feature of FLOX-LPG propellant combinations is that maximum theoretical impulse occurs at stoichiometric mixture ratios, with attendant maximum combustion temperatures. Most other propellant combinations have maximum theoretical impulses at fuel-rich mixture ratios, with correspondingly reduced combustion temperatures. Because of this feature, FLOX-LPG engines have two unique problems to overcome, besides all the typical problems that other engines have. These two problems are

- (1) High combustion temperatures (7300°R (4055 K) experimental)
- (2) The necessity of reacting completely both propellants; not just the oxidizer as in the case of fuel-rich design mixture ratios

Solution of the first problem is a materials problem, further complicated by the chemi-

cal reactivity of the combustion gases. The second problem requires careful design of the injector to achieve high combustion efficiencies in reasonable chamber lengths with reasonable injection pressure drops. The high-efficiency injector must also be free of combustion instability, and streaking, so as not to further aggravate the chamber materials problem.

In view of the difficulties encountered in designing regeneratively cooled FLOX-LPG propulsion systems (ref. 1), the NASA Lewis Research Center has undertaken an in-house task of designing and testing an ablatively cooled FLOX-propane rocket engine. The objective of the program was to design and test fire a rocket engine which would demonstrate stable combustion at a delivered characteristic exhaust velocity efficiency of 95 percent at 100-psia (689-kN/m^2) chamber pressure and an O/F of 4.5. Various candidate ablative materials were selected to provide a continuous firing duration of 300 seconds. A hard throat insert design was considered for use where ablative materials could not provide erosion-free operation. An additional objective was to determine materials limitations by varying chamber pressure and O/F.

The scope of the program included engine operation at chamber pressures from 100 to 200 psia (689 to 1378 kN/m^2), an O/F range of 3.5 to 5.0 with a throat diameter of 1.2 inches, and an expansion area ratio of 2.0 (sea-level operation). The thrust generated was 150 to 300 pounds force (667 to 1334 N) when corrected for vacuum.

APPARATUS

Engine Design

The initial design operating conditions were chosen as an oxidant-to-fuel mixture ratio of 4.5 to 1, chamber pressure of 100 psia (689 kN/m^2), and a throat diameter of 1.2 inches (3.05 cm); these being typical of pressure-fed rocket engines of the 150-pound- (667-N -) thrust size. The nominal engine design values included a characteristic length L^* of 33 inches (83.8 cm) and a contraction ratio of 3.0. The contraction ratio was selected as the minimum value to prevent excessive ablative erosion in the chamber section. Four different types of injector designs were selected to provide a range of injection variables within which both ablative compatibility and high performance could be attained. The injectors were first evaluated with water-cooled chambers and nozzles. A range of ablative materials was selected for evaluation, with the emphasis on graphitic materials thought to be compatible with the FLOX-propane combustion environment. A graphite throat insert was also designed and fabricated for use if ablative materials suffered excessive throat erosion.

Injectors. - As noted earlier, the FLOX-LPG propellants are unique in that theo-

retical performance is predicted to peak at the stoichiometric mixture ratio if the reaction products are HF and CO. Most contemporary propellant combinations peak on the fuel-rich side of stoichiometric. With FLOX-LPG, both propellants must be completely reacted to provide maximum performance at the theoretical peak. Thorough mixing of propellants is thus required to assure utilization of each molecule.

Because of the extremely high combustion temperature of FLOX-propane (7300°R) and the highly reactive fluorine in the combustion products, attack on standard graphite ablative materials was considered to be a problem. For this reason, some of the injectors were designed to provide fuel-rich boundary layers for ablative protection.

The use of ablative thrust chambers with earth-storable propellants has sometimes necessitated a compromise between ablative erosion and injector performance level. (One such propellant is a 50-50 blend of unsymmetrical dimethyl hydrazine and anhydrous hydrazine with nitrogen tetroxide.) The injectors designed for this use were intended to encompass the range of values necessary to assure ablative protection as well as high ηC^* performance if possible.

Four basic injector configurations were designed for the nominal test conditions. All of the injectors were designed to operate with both propellants in the liquid state through the injection elements. The designs were compatible with pressure-fed engine systems which require low-pressure-drop components. A maximum injector pressure drop of 50 psi (345 kN/m^2) was selected for the nominal design condition. An oxidant-to-fuel velocity ratio similar to that providing maximum performance with the previously mentioned earth-storable propellant (0.6 to 0.8) was considered applicable because both combinations are hypergolic and both combinations have oxidant densities of about 90 pounds per cubic foot (1441 kg/m^3) and fuel densities of about 50 pounds per cubic foot (801 kg/m^3). A ratio of oxidant-to-fuel orifice diameter near 1 was thought to be a desirable objective for unlike impingement, in order to assure good mixing of fuel and oxidant. Calculations made by the method of reference 2 indicated 0.020-inch- (0.051-cm-) diameter parallel fuel jets would be 99 percent vaporized in an 8-inch (20.3-cm) chamber length. Due to the low fuel flow (0.101 lb/sec (0.0458 kg/sec)), we were able to use the smallest standard drill size (0.0135 in. (0.0342 cm)) for all the injector designs and still maintain injector pressure drop values of the order of 50 psi (345 kN/m^2). These small orifices should assure complete fuel vaporization in the chamber length (10.5 in. (26.7 cm)) used for the nominal engine ($L^* = 33\text{ in. (83.8 cm)}$). Oxidant vaporization was not thought to be limiting, and calculation indicated that 0.070-inch- (0.178-cm-) diameter impinging oxidant streams would be 95 percent vaporized in the nominal engine ($L^* = 33\text{ in. (83.8 cm)}$). Table I lists the injector design values for each configuration.

Injector 1 (an oxidant doublet - fuel showerhead type) consisted of 10 oxidant doublet elements and 46 fuel showerhead elements. The injector pattern is shown in figure 1.

TABLE I. - INJECTOR DESIGN PARAMETERS

[Chamber pressure, 100 psia (689 kN/m²); throat diameter, 1.2 inches (3.05 cm); FLOX-propane; oxidant-to-fuel ratio, 4.5.]

Injector ^a	Oxidant at 140 ^o R							Fuel at 200 ^o R							Velocity ratio, v _{ox} /v _f	Diameter ratio, D _{ox} /D _f	Momentum ratio, W _f v _f /W _{ox} v _{ox}
	Number of holes	Hole diameter		Pressure change, ΔP (C _d =0.7)		Injection velocity, v _{ox}		Number of holes	Hole diameter		Pressure change, ΔP (C _d =0.7)		Injection velocity, v _f				
		in.	cm	psi	kN/m ²	ft/sec	m/sec		in.	cm	psi	kN/m ²	ft/sec	m/sec			
1	20	0.035	0.0889	28	193	37	11.3	46	0.0135	0.0342	24	165	50	15.2	0.74	2.59	0.300
2	52	.021	.0533	32	221	40	12.2	26	↓	↓	78	547	89	27.1	.45	1.55	.494
2a	52	.026	.0660	13	89.6	26	7.9	26	↓	↓	78	547	89	27.1	.29	1.93	.766
3, 4, 5	36	.0225	.0572	53	365	50	15.2	37	↓	↓	39	268	62	18.9	.81	1.67	.274
5a	36	.026	.0660	28	193	32	9.8	37	↓	↓	39	268	62	18.9	.52	1.93	.427
6	74	.018	.0457	29	200	38	11.6	37	↓	↓	39	268	62	18.9	.613	1.33	.363

^aInjector descriptions:

Injector 1 - oxidant doublet - fuel showerhead type

Injector 2 - circular-pattern oxidant-fuel-oxidant triplet

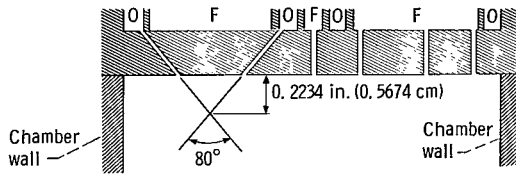
Injector 3, 4, 5 - circular-pattern, fuel-oxidant-oxidant-fuel split triplets:

3 - fuel cooled; electrodeposited face

4 - fuel cooled; electron-beam-welded face

5, 5a - oxidant cooled; brazed face

Injector 6 - mutually perpendicular oxidant-fuel-oxidant triplet



Ring	Ring diameter		Pro- pel- lant	Num- ber of holes	Hole diameter	
	in.	cm			in.	cm
Center	0	0	F	1	0.0135	0.0342
1	.500	1.27	F	5	.0135	.0342
2	.750	1.91	O	10	.0350	.0889
3	1.250	3.18	F	10	.0135	.0342
4	1.500	3.81	O	10	.0350	.0889
5	1.750	4.45	F	30	.0135	.0342
Wall	2.080	5.28	--	--	--	--

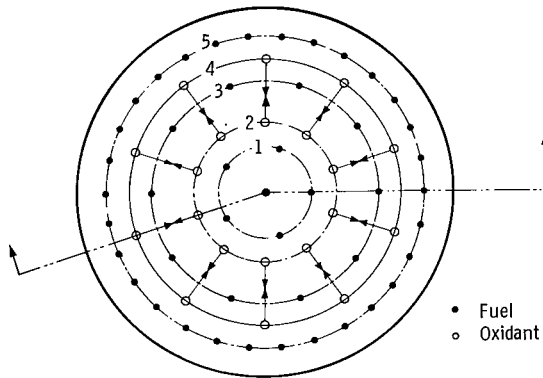
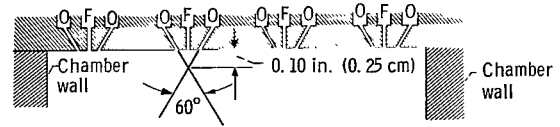


Figure 1. - Injector 1 (oxidant doublet - fuel showerhead type).



Ring	Ring diameter		Pro- pel- lant	Num- ber of holes	Hole diameter	
	in.	cm			in.	cm
Center	0	0	--	0	--	--
1	.428	1.087	O	8	0.0210	0.0533
2	.544	1.382	F	8	.0135	.0342
3	.659	1.674	O	8	.0210	.0533
4	1.516	3.851	O	18	.0210	.0533
5	1.632	4.15	F	18	.0135	.0342
6	1.747	4.437	O	18	.0210	.0533
Wall	2.080	5.28	--	--	--	--

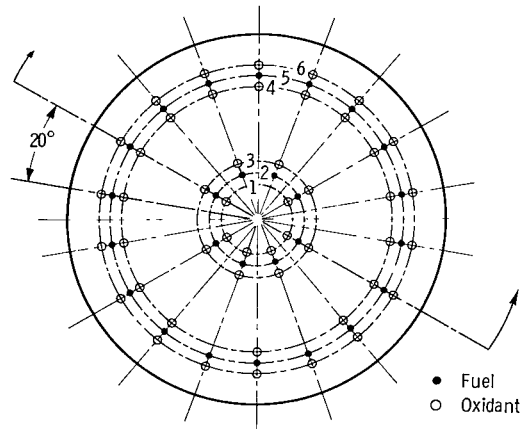
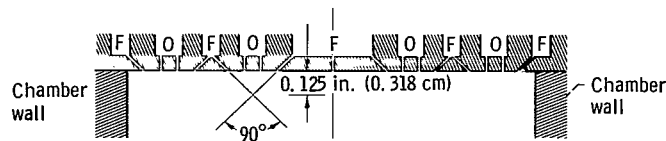


Figure 2. - Injector 2 (circular-pattern oxidant-fuel-oxidant triplet).

The fuel showerheads were small (0.0135-in. (0.0342-cm) diam) to facilitate fuel vaporization. Ten of the fuel showerheads were placed so as to intersect the fans formed by the oxidant doublets. An outer ring of fuel holes was used to provide a fuel-rich zone on the chamber and nozzle walls.

Injector 2 was a 26-element, circular-pattern, oxidant-fuel-oxidant triplet injector. The injector pattern is shown in figure 2. The design was derived using an existing showerhead injector, so that manifold placement dictated element ring spacing. The oxidant-fuel-oxidant configuration was used to keep the diameter of the oxidant holes (0.021 in. (0.0533 cm)) close to the diameter of the fuel holes (0.0135 in. (0.0342 cm)). This resulted in an oxidant-to-fuel velocity ratio of 0.45.

Injectors 3, 4, and 5 (circular-pattern, fuel-oxidant-oxidant-fuel split triplets) were similar to each other except for the materials of construction and the injector face coolant used. The injector pattern is shown in figure 3. The design was derived from a



Ring	Ring diameter		Pro- pel- lant	Num- ber of holes	Hole diameter	
	in.	cm			in.	cm
Center	0	0	F	1	0.0135	0.0342
1	.550	1.397	F	6	.0135	.0342
2	.720	1.829	O	↓	.0225	.0572
3	.880	2.235	O		.0225	.0572
4	1.050	2.667	F	↓	.0135	.0342
5	1.390	3.531	F		.0135	.0342
6	1.560	3.962	O	↓	.0225	.0572
7	1.720	4.369	O		.0225	.0572
8	1.890	4.801	F	↓	.0135	.0342
Wall	2.080	5.280	--	--	---	---

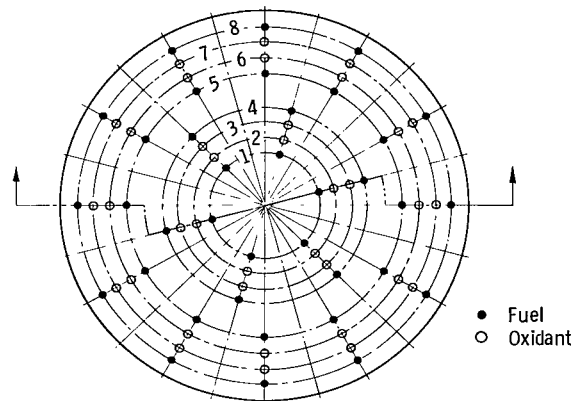


Figure 3. - Injectors 3, 4, and 5 (circular-pattern fuel-oxidant-oxidant-fuel split triplet). Injector 3, fuel-cooled, electrodeposited nickel face; injector 4, fuel-cooled, electron-beam-welded nickel face; injector 5, oxidant-cooled, brazed nickel face.

Bell Aerosystems concept which replaced the center oxidant hole of a conventional fuel-oxidant-fuel triplet with two parallel oxidant holes, hence the name split triplet. The concept gives fuel-on-oxidant impingement followed by impingement of the resultant fans for axial momentum. Given a fuel hole diameter of 0.0135 inch (0.0342 cm), the oxidant diameter was chosen to provide an oxidant-to-fuel velocity ratio of 0.81. The pattern was circular with 18 element groups and an extra fuel hole in the center for improved local face cooling. The pattern was intended to provide uniform element distribution over the face area with the exception of the center.

Injector 6 was a 37-element, oxidant-fuel-oxidant triplet. The triplets were arranged to be mutually perpendicular as shown in figure 4. The design was similar to successful arrangements used with earth-storable propellants (ref. 3). Hole diameters of 0.0135 inch (0.0342 cm) for fuel and 0.018 inch (0.046 cm) for oxidizer were used in

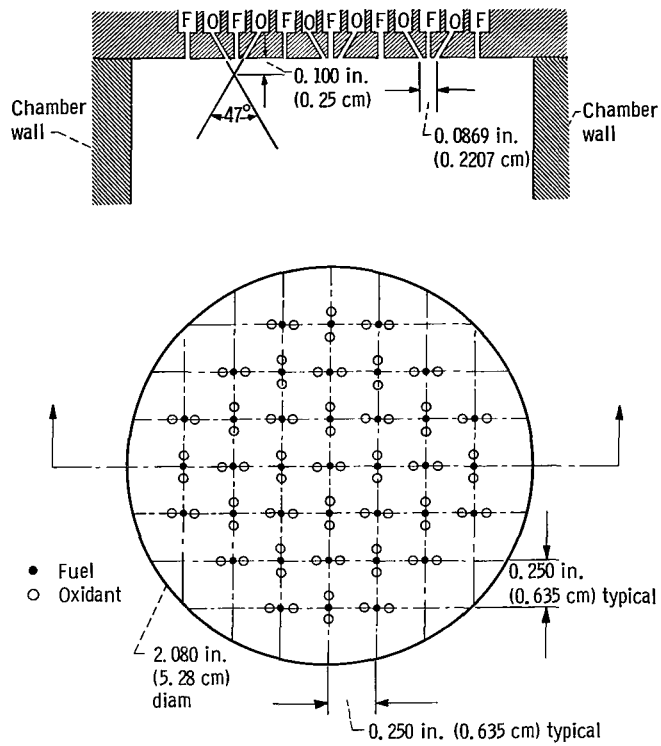
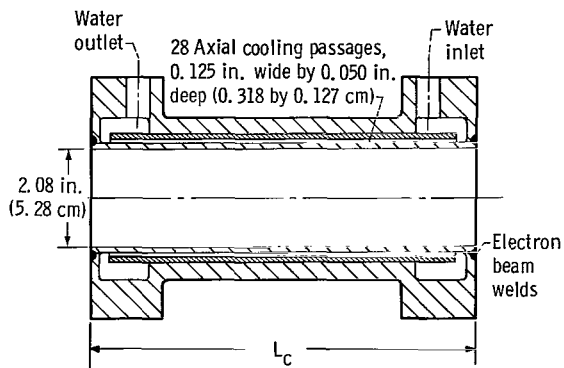


Figure 4. - Injector 6 (mutually perpendicular oxidant-fuel-oxidant triplet); 37 fuel holes 0.0135 inch (0.0342 cm) in diameter; 74 oxidant holes 0.018 in. (0.0457 cm) in diameter.



Chamber length, L_c		Characteristic engine length, L_E^*	
in.	cm	in.	cm
4	10.16	21	53.3
8	20.3	33	83.8
12	30.5	51	129.5

Figure 5. - Design of water-cooled chamber. Material, 5083 aluminum.

order to provide good vaporization. The perpendicular triplets were used to provide good mixing.

Water-cooled chambers. - Water-cooled chambers were designed according to the drawing of figure 5. The design was intended to cool at a heat-flux level of 6 Btu per square inch per second ($9800 \text{ kW}/(\text{m}^2)(\text{sec})$). The water-cooled chambers were used to evaluate injector performance in the various lengths shown. The L_E^* values include the nozzle section to give an overall value. The 8-inch- (20.3-cm-) long water-cooled chamber was also used with the ablative chamber-nozzle sections.

Water-cooled chamber-nozzle combinations. - A water-cooled chamber-nozzle was designed as shown in figure 6. The design was also intended to cool at a heat-flux level of 6 Btu per square inch per second ($9800 \text{ kW}/(\text{m}^2)(\text{sec})$) and was used with the water-cooled chambers during injector evaluation.

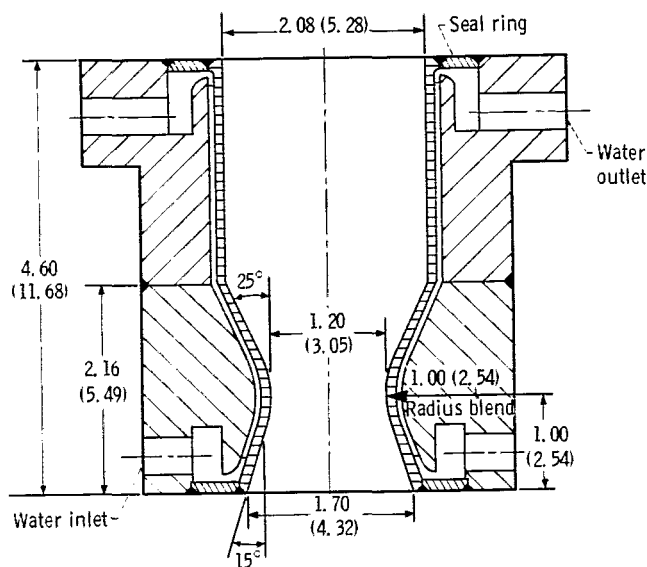


Figure 6. - Water-cooled nozzle. Material, 1100 aluminum. Dimensions are in inches (cm).

Ablative chamber-nozzle combinations. - Unlike the earth-storable propellant environment, where experimental combustion temperature is about 5200°R , the FLOX-propane experimental combustion temperature is about 7300°R . Because of this high combustion temperature, the surface would be expected to reach the melting temperature of silica (3600°R) very rapidly, so that ablative materials containing silica would be expected to erode very quickly as a result of melting of the silica reinforcement.

Unlike silica, graphite does not melt but begins to vaporize at approximately 6500°R . The vaporization rate is a function of the material temperature and partial

pressure of the various constituents in the boundary layer. Erosion of the graphite-phenolic was, therefore, expected to be controlled primarily by fluorine and oxygen thermochemical attack rather than by graphite vaporization. Another possible mode of erosion, particularly at the nozzle throat, would be mechanical removal of the ablative structure by the local stream shear forces.

The combustion products of FLOX-propane are considerably less oxidizing than the combustion products of earth-storable propellants. Carbons and graphites oxidize catastrophically in the earth-storable propellant combustion environment (ref. 3), but it was thought oxidation would be less of a problem in the FLOX-propane combustion environment. Therefore, ablative chamber-nozzles made of graphitic materials were expected to perform quite well. The intent was to control thermochemical attack by providing local mixture-ratio control. The only causes of failure should then be of a structural nature; such as thermal shock, or surface erosion because of shear failure. Hard throat inserts would be used to overcome erosion problems caused by possible structural failures of the ablatives.

An ablative chamber-nozzle, shown in figure 7(a), was used to evaluate the long-term firing capability of a flight-weight design at 100-psia (689 kN/m^2) chamber pressure. The cylindrical section was incorporated to evaluate the effect of unburned propellant and O/F variations on the ablative material upstream of the converging nozzle.

Table II lists the various materials tested, and their constituents where known. Most of the materials were obtained from nozzle fabricators using the manufacturers' specifications listed for procurement purposes.

Silica cloth - phenolic ablative material was included as a reference material because of its wide use with earth-storable propellants. Some preliminary plasma tests and computer predictions also indicated that silica-reinforced plastics might perform satisfactorily in the test environment (ref. 4).

The molded nozzles (3 and 4 in table II) were used to evaluate potential low-cost nozzle materials in the high-temperature environment of FLOX-propane combustion.

Ablative chamber-nozzle with throat insert. - Figure 7(b) shows the design of an ablative chamber nozzle with a hard throat insert of ATJ graphite. The insert and chamber liner were made from commercial-grade graphite materials to serve as a standard of comparison with other test environments. They were intended for use when ablative materials would not provide throat erosion resistance.

TABLE II. - ABLATIVE MATERIALS TESTED

Material	Specification number	Reinforcement				Binder	
		Material	Form	Orientation angle, deg	Content, wt. %	Material	Content, wt. %
1	FM5020	Silica	Cloth	30	70	Phenolic	30
2	MXSC195	50 Percent silica - 50 percent carbon	Cloth	(a)	55	Phenolic	45
3	T4120, 1000-psia (6890-kN/m ²) molding	Proprietary low-cost graphite compounds					
4	T4120, vacuum bag molding						
5	FM5055A	Carbon	Cloth	60	65	Phenolic	35
6	FM5064	Graphite	Cloth	60	65	Phenyl aldehyde resin	35

^a1/2- by 1/2-in. (1.27- by 1.27-cm) squares.

Facility

Test cell. - The experimental test firing runs were conducted in the rocket engine test facility shown in figure 8. A schematic diagram of the installation is given in figure 9. The engine and bedplate assembly was suspended by flexural members to allow freedom of motion in the axial direction for thrust measurement.

The propane tank was surrounded by liquid nitrogen pressurized at 100 psia (689 kN/m²) to provide a propellant temperature of 180° R (100 K) in the tank. Some pressure was necessary to keep the liquid nitrogen above the freezing temperature of propane (152° R (84 K)), and 180° R (100 K) was selected as a value which allowed relatively stable fuel-injection temperatures during a long ablative firing.

FLOX was prepared by mixing liquid oxygen and liquid fluorine in a liquid-nitrogen-jacketed weigh tank. The average value obtained by the weigh method was 76.2-percent F₂ with a standard deviation of ±0.8-percent F₂. The actual values obtained during each mixing operation were used for data analysis. Samples actually varied between 75- and

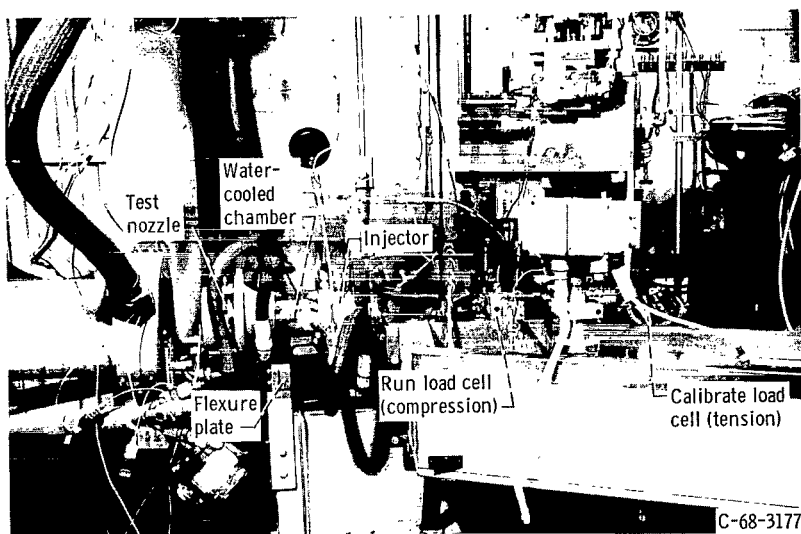


Figure 8. - Test facility.

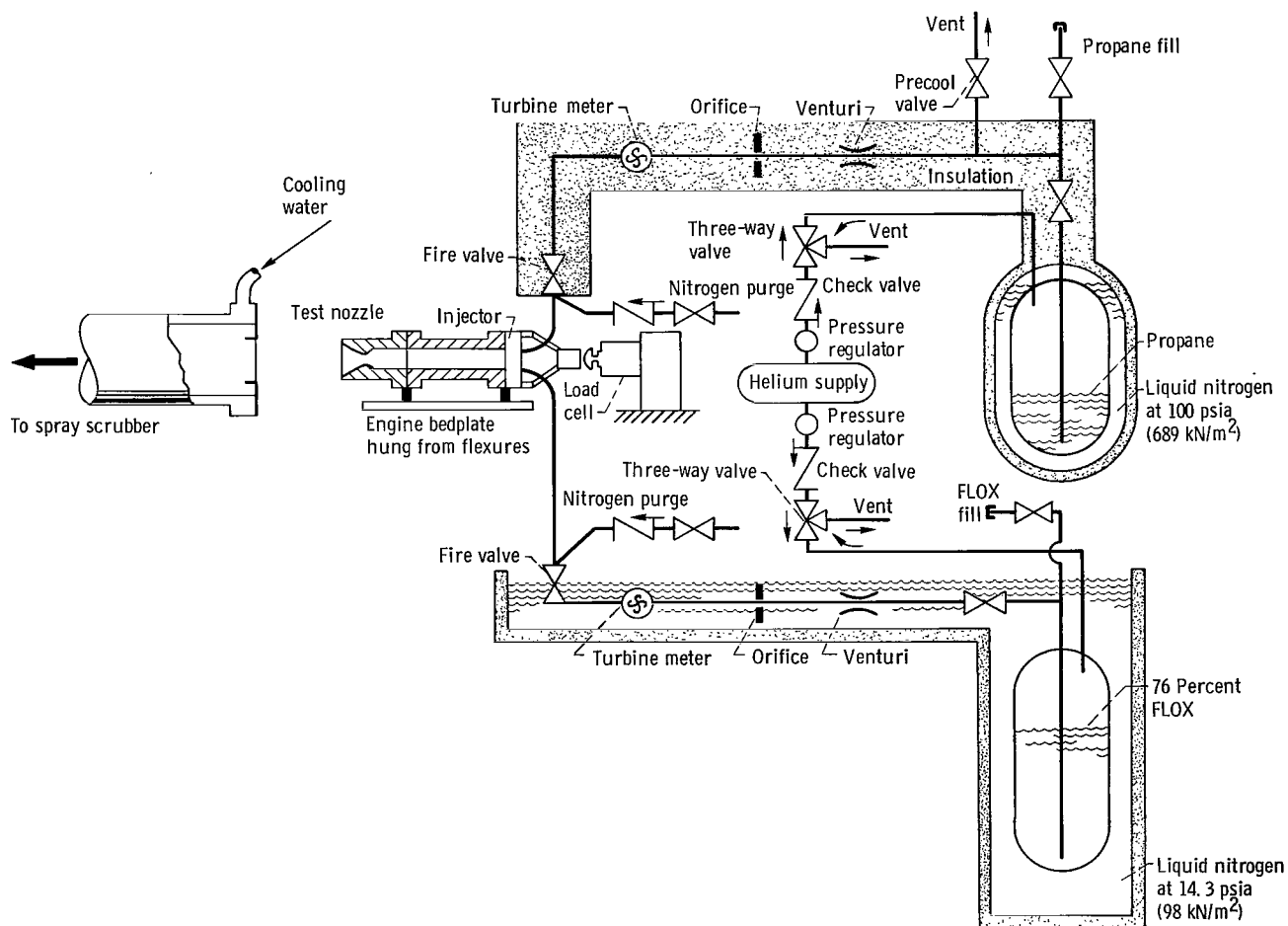


Figure 9. - Schematic diagram of test installation.

78-percent fluorine. Each batch was assumed to be mixed after introduction of the two liquids followed by tank trailer transfer to the test site. The percentages were also checked by analyzing a sample taken during each transfer. The sample was trapped in a liquid-nitrogen bath and analyzed by the mercury absorption technique of reference 3. The standard deviation obtained from the samples was ± 2.38 -percent F_2 , indicating problems in the sampling technique.

Instrumentation. - Chamber pressure was measured by redundant, strain-gage bridge-type pressure transducers closely coupled to a hole in the injector face (fig. 10). A high-frequency-response piezoelectric transducer mounted flush with the chamber wall was used to monitor for combustion instability.

Thrust measurements were made with a double-bridge, strain-gage load cell loaded in compression. The run load cell was calibrated against a standard load cell in tension. A hydraulic cylinder provided the calibration force.

The flow rate of each propellant was measured with venturi, orifice, and turbine meters arranged in series. Each meter was calibrated separately with water flow in a weigh tank facility. The calibrations were then adjusted for propellant densities and thermal contraction. Three meters were used to provide redundancy of measurement and a method for checking flow rates against one another. Since the meters were not calibrated with the actual cryogenic propellants but only with water, propellant flow rates contained a degree of uncertainty. The three different types of meters were used to cancel out problems and anomalies in calibrating orifices, turbines and venturis, as well as in converting to actual propellant flows. The three fuel flowmeters agreed within ± 2 percent of one another while the three oxidant meters agreed within ± 1.5 percent of one another. The average value was used for each propellant.

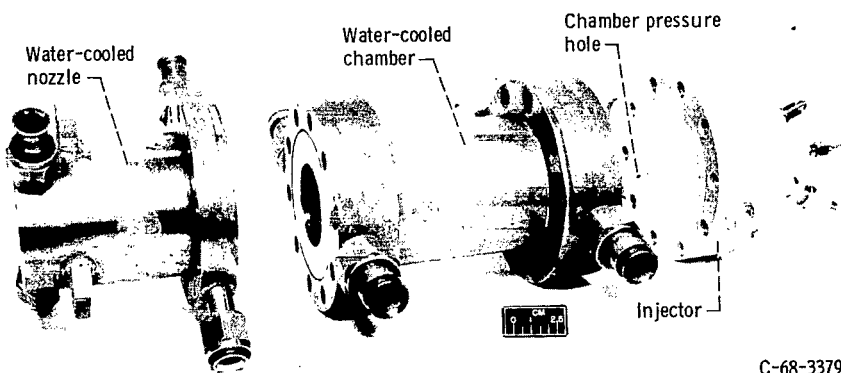
Propellant temperatures were measured with platinum resistance elements arranged in a bridge circuit and calibrated over the temperature range of interest. The range for fuel was 160° to 240° R (89 to 133 K), and the range for oxidant was 138° to 148° R (77 to 82 K).

Data recording and processing. - All electrical sensor outputs were sampled at the rate of 4000 samples per second, digitized, and recorded on magnetic tape. The digital data were converted into engineering quantities by use of a digital computer. Selected sensor outputs were recorded continuously on strip charts and an oscillograph for system monitoring and control room processing.

PROCEDURE

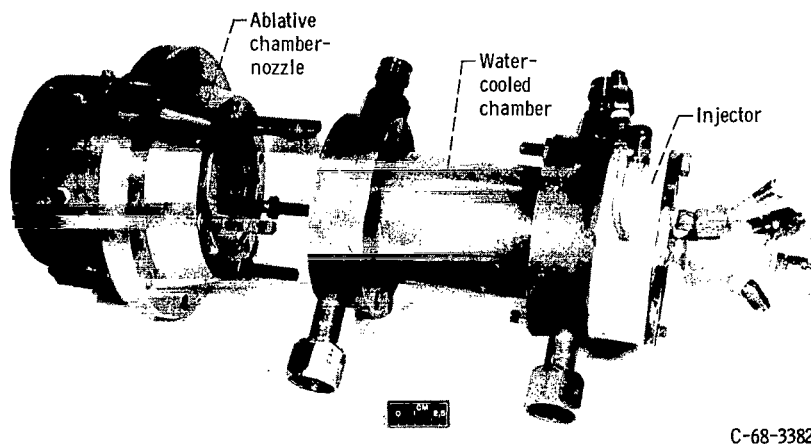
Engine Assembly

Figure 10 illustrates the injector test assembly with a water-cooled chamber and nozzle. The assembly used to test an ablative material is shown in figure 11.



C-68-3379

Figure 10. - Water-cooled nozzle and chamber with injector.



C-68-3382

Figure 11. - Ablative chamber-nozzle, water-cooled chamber, and injector.

Test Procedure

The instrumentation was electrically calibrated prior to each run. A sequence timer automatically activated appropriate valves, data acquisition equipment, and propellant line purges. Precooling of the fuel line was accomplished by running liquid propellant through the line prior to firing. Three-fourths of the total line length was cooled in this manner. A high-frequency, flush-mounted pressure transducer located in the chamber was monitored with an oscilloscope, and the data were recorded on magnetic tape. During each firing, O/F and chamber pressure were held constant by separate closed-loop controllers. Thus, if throat erosion occurred, propellant flow rate was increased to maintain constant chamber pressure.

Throat area was determined after testing by tracing an outline of the throat as projected by a 10-power optical comparator. The area of the projection was measured with a planimeter and the result converted to an effective throat radius.

RESULTS AND DISCUSSION

Injector Evaluation

All of the injector designs were tested with water-cooled chambers and nozzles to measure characteristic exhaust velocity efficiency and to assure injector durability. Table III lists the delivered performance and important injector parameters.

Possible corrections to the delivered performance include heat losses to the water-cooled chamber, friction losses, and throat area changes caused by thermal effects. The heat-loss value calculated from the enthalpy rise of the water could add 2.1 percent to the ηC^* values reported. The other losses were neglected.

Figure 12(a) is a plot of ηC^* for injector 1 (an oxidant doublet - fuel showerhead injector). To illustrate the magnitude of the heat-loss correction, both values are shown in figure 12(a). Hereinafter, only uncorrected values are shown in the figures. The delivered efficiency of 88.5 percent at an O/F of 4.5 did not meet the required 95-percent level. This injector was tested during attempts to use fuel stored in a water bath at 510° R. As the pressure drop in table III indicates, liquid was not maintained through the injector with the propane stored at 510° R. We felt that use of colder fuel with this injector would result in even lower performance. The oxidant fans were not able to vaporize and mix with the fuel showerheads sufficiently. The most likely reason for the low performance was the uneven distribution of fuel and oxidizer at the injector face. Figure 1 illustrates an outer ring of fuel showerheads intended to provide a fuel-rich boundary layer, which undoubtedly detracted from performance. If different mani-

TABLE III. - INJECTOR PERFORMANCE COMPARISON

[Chamber pressure, 100 psia (689 kN/m²); throat diameter, 1.2 inches (3.05 cm);
FLOX-propane fuel; oxidant-to-fuel ratio, 4.5; oxidant temperature,
140° R (77.8 K).]

Injector	Type	Oxidant pressure change, ΔP_{ox}		Fuel				Characteristic exhaust velocity efficiency, ηC^* , percent
				Pressure change, ΔP_f		Temperature		
		psi	kN/m ²	psi	kN/m ²	°R	K	
1	Oxidant-doublet-fuel showerhead, circular pattern	43	296	143	986	520	288	88.5
2	Oxidant-fuel-oxidant triplet, circular pattern	119	820	92	634	290	161	92.2
2a		51	352	49	338	200	111	93.0
3	Fuel-oxidant-oxidant-fuel split triplet, circular pattern	42	290	31	214	200	111	92.8
4		53	366	37	255	200	111	91.5
5		63	434	41	283	200	111	93.5
5a		25	172	45	310	200	111	91.8
6	Oxidant-fuel-oxidant, mutually perpendicular	68	317	37	255	200	111	95.5

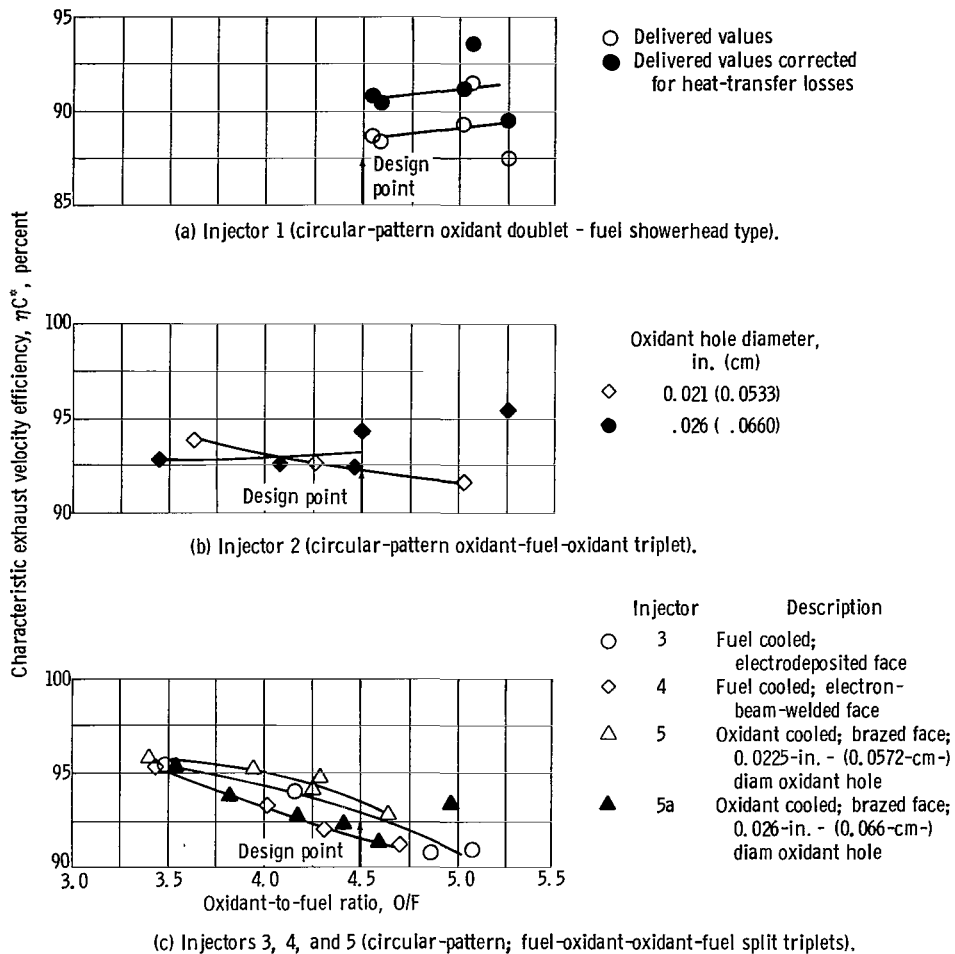


Figure 12. - Performance against oxidant-to-fuel ratio for various injectors. Chamber pressure, 100 psia (689 kN/m²); throat diameter, 1.2 inches (3.05 cm); characteristic engine length, 33 inches (83.8 cm); FLOX-propane fuel.

folding had been available, the single ring of oxidant doublets could have been made into three rings to provide better distribution and increased performance.

Figure 12(b) is a plot of η_{C^*} for injector 2 (a circular-pattern oxidant-fuel-oxidant triplet). The efficiency of 92 percent at an O/F of 4.5 was below the required 95-percent level. The fan orientation was such that oxidant-rich areas coincided with oxidant-rich areas on adjacent fans, causing nonuniform O/F distribution. Inspection of the injector pattern (fig. 2) shows that the elements are not distributed uniformly across the face - a feature previously determined to be desirable for providing uniform mass distribution. This injector was derived from an existing showerhead design so that optimum spacing of the elements was not possible.

A modification to injector 2 involved enlarging the oxidant holes from 0.021 to 0.026 inch (0.0533 to 0.066 cm) diameter. The intent was to increase the momentum

ratio as indicated in reference 3. As figure 12(b) indicates, no significant improvement was achieved by increasing the momentum ratio.

Figure 12(c) compares the ηC^* for injectors 3, 4, and 5 (circular-pattern, fuel-oxidant-oxidant-fuel split triplets). For injector 3, the efficiency of 93 percent at an O/F of 4.5 was below the required 95-percent level, although 95-percent efficiency was achieved at an O/F of 3.5. The pattern was arranged in two rings with the inner elements spaced midway between the outer elements (see fig. 3). This arrangement impinged oxidant-rich fan areas on oxidant-rich fan areas of adjacent elements and also allowed the resultant fans to circulate unimpeded. Mixing was apparently not sufficient, although a lower oxidant-to-fuel-mixture ratio improved efficiency. The electrodeposited face of injector 3 was buckled during testing. The faceplate of injector 4 was electron beam welded to avoid the structural problems found with electrodeposited faceplates. The efficiency of 91.5 percent at an O/F of 4.5 was somewhat lower than that of injector 3. No structural deterioration was noted, which indicated the electron-beam-welded face was an improvement over the electrodeposited nickel face. Injector 5 was the same as injector 3 except the face was installed by brazing and was oxidizer cooled. A slightly higher efficiency of 93.5 percent at an O/F of 4.5 was still below the desired level of 95 percent. Cooling and construction were adequate, however. The minor differences in performance among the three identical patterns were most likely due to minor variations in fuel and oxidizer velocities caused by different face cooling techniques or injector face warpage.

Previous work, reported in reference 1, indicated that increasing the fuel-to-oxidizer momentum ratio could increase the ηC^* . The data for injector 5 appear to confirm this trend when the O/F variation data are replotted, as in figure 13. It was decided to increase the momentum ratio by enlarging the oxidant holes from 0.0225 to

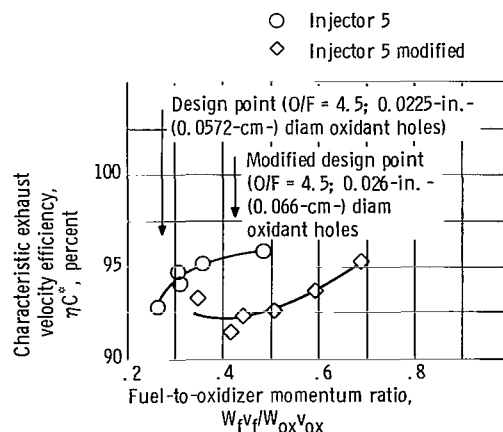


Figure 13. - Injector 5 performance comparison. Momentum ratio varied for each design by varying oxidant-to-fuel ratio.

0.026 inch (0.0572 to 0.0660 cm). The results are shown in figures 12(c) and 13. The differences in momentum ratio shown for each set of symbols in figure 13 was due to O/F variation rather than injector changes. The difference between injectors is characterized by the difference between the lines. The increased momentum ratio actually decreased ηC^* . We did not consider the decreased efficiency was caused by poorer oxidizer vaporization because the fuel was assumed to be limiting, and from calculations described previously, 0.070-inch- (0.178-cm-) diameter oxidant holes would provide satisfactory vaporization. For this particular injector, a ratio of oxidant hole diameter to fuel hole diameter of 1.93 gave ηC^* of 92 percent at an O/F of 4.5. A diameter ratio of 1.67 gave ηC^* of 93.5 percent at an O/F of 4.5. These results indicate that a diameter ratio approaching 1 would give increased ηC^* . The increased oxidizer hole size decreased the oxidizer velocity, which permitted O/F distribution and radial mass flux such that performance decreased and gouging of the chamber walls occurred (see fig. 14). The major gouges appeared to be where the resultant vectors from the inner row of elements reinforced the resultant vectors from the outer row of elements. The mixture-ratio distribution parameter, as reported in reference 5, does not provide an adequate guide for this type of injector, probably because that work on unlike doublets does not apply to the split triplet injector.

Figure 15(a) is a plot of ηC^* for injector 6, an oxidant-fuel-oxidant triplet injector with the elements mutually perpendicular. The value of 95.5 percent at an O/F of 4.5 met the objectives of the program. A further test series showed a slight increase in performance at 200-psia (1378-kN/m²) chamber pressure. The better performance of injector 6 compared to injector 2 (also oxidant-fuel-oxidant triplet) was primarily due to the perpendicular orientation of the elements with respect to one another and the attendant

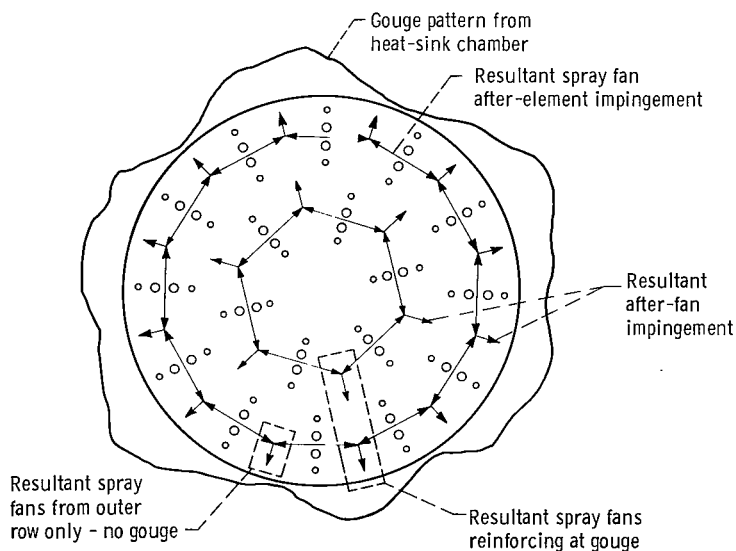
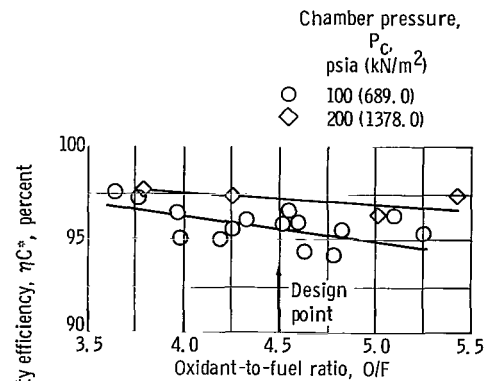
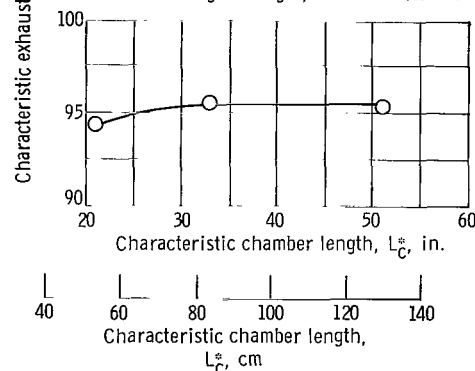


Figure 14. - Injector 5; modified, recirculation pattern.



(a) As function of oxidant-to-fuel ratio. Characteristic engine length, 33 inches (83.8 cm).



(b) As function of characteristic chamber length. Chamber pressure, 100 psia (689 kN/m²); oxidant-to-fuel ratio, 4.5.

Figure 15. - Performance of injector 6 (mutually perpendicular oxidant-fuel-oxidant triplet type). Throat diameter, 1.2 inches (3.05 cm); FLOX-propane fuel.

better mixing obtained (ref. 3). Also contributing to the improvement was the more uniform element distribution, which gave more uniform mass distribution, and smaller oxidant holes, which gave better propellant vaporization.

Further characterization of injector 6 included L^* variation, which produced the results shown in figure 15(b). No significant increase in ηC^* was noted at an L^* of 51 inches (129.5 cm) but a slight decrease was noted at a value of 21 inches (53.3 cm). It was concluded that an L^* of 33 inches (83.8 cm) was sufficient to adequately vaporize and burn the propellants.

During performance testing with water-cooled chambers, no predominant high frequency was detected during steady-state engine operation. It was therefore concluded that there was no combustion instability. Normal minor fluctuations in chamber pressure during steady-state operation were generally 2 to 3 percent of chamber pressure in magnitude.

Water-Cooled Chamber and Nozzle Evaluation

During performance testing of all the injectors, a deposit of amorphous carbon (soot) formed on the walls of the water-cooled chamber and nozzle. The layer was a few thousandths of an inch thick and was removed easily by wiping. All of the injectors produced some carbon deposition on the water-cooled chambers over the entire range of O/F values tested.

Average heat-flux values were determined from the enthalpy rise of the water. The range of values of heat flux was 2.0 to 3.0 Btu per square inch per second (3200 to 4800 kW/(m²)(sec)) for both chamber and nozzle. An average value of 2.5 Btu per square inch per second (4000 kW/(m²)(sec)) was used to calculate η_{C^*} losses to the water-cooled engine.

Ablative Material Evaluation

The ablative material evaluation was performed with injector 6. A water-cooled chamber section was used in conjunction with the ablative chamber (see fig. 11, p. 15) so that the engine L^* was 33 inches (83.8 cm).

Ablative material performance. - Figure 16 compares the zero erosion time and the total firing time of a variety of ablative materials at a chamber pressure of 100 psia (689 kN/m²) and an O/F of 4.5. Testing was terminated when steady-state erosion was

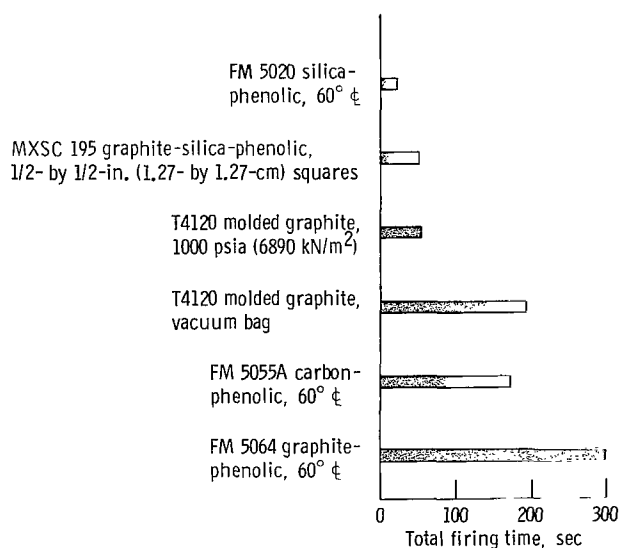
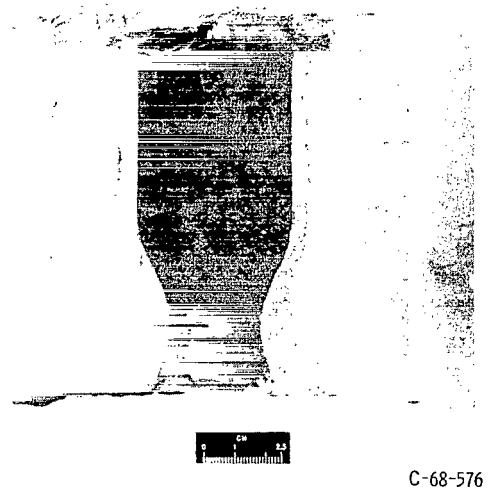
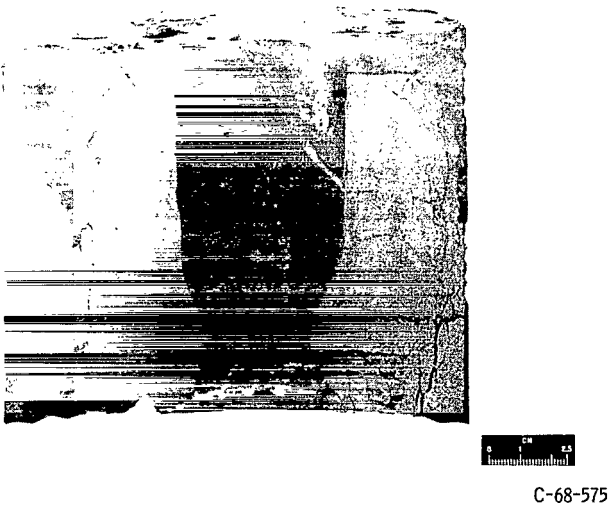
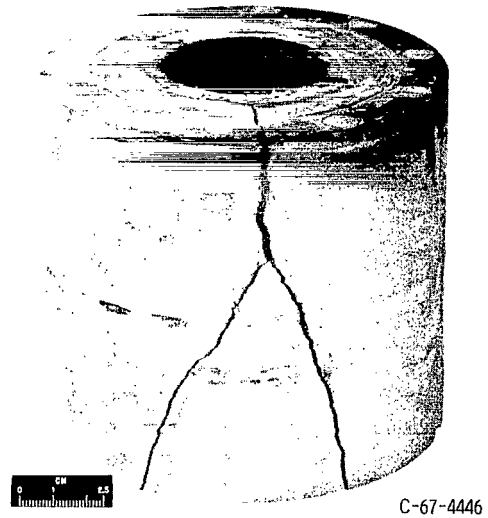
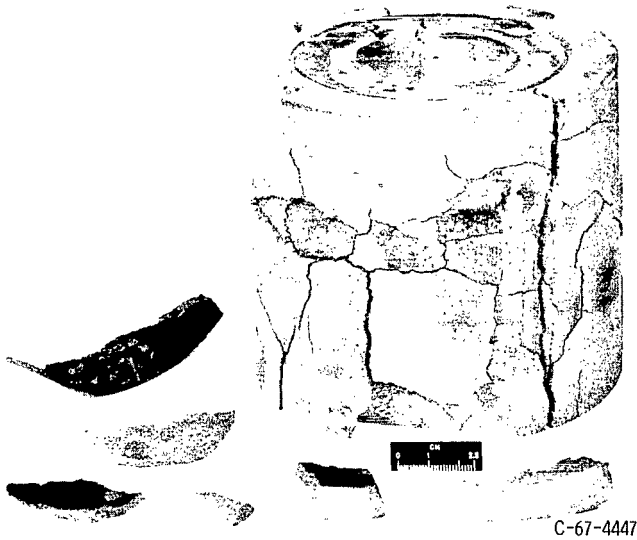


Figure 16. - FLOX-propane ablative performance. Injector 6 (37-element oxidant-fuel-oxidant triplet); chamber pressure, 100 psia (689 kN/m²); oxidant-to-fuel ratio, 4.5. Shaded portion represents zero erosion time.

established, when an emergency condition arose, or when the 300-second firing goal was reached.

Silica cloth - phenolic resin ablative material began to erode after 6 seconds. This erosion was due to melting of the silica reinforcement as was expected in the high-temperature FLOX-propane combustion environment.

A material reinforced with 1/2- by 1/2-inch (1.27- by 1.27-cm) squares of a cloth containing a filament composed of graphite and silica began to erode after 10 seconds. The graphite was not present in sufficient quantity to offset the melting of the silica,



(a) T4120 - vacuum bag molding after 193-second run.

(b) T4120 - 1000-psia (6890 kN/m^2) molding pressure after 55-second run.

Figure 17. - Two low-cost molded graphite (T4120) chambers. Chamber pressure, 100 psia (689 kN/m^2); oxidant-to-fuel ratio, 4.5.

which left the graphite unsupported and subject to mechanical removal.

Two low-cost molded graphite (T4120) chamber nozzles were evaluated - one molded at vacuum bag pressure and the other molded at 1000 psia (6890 kN/m^2). The lower density material molded at vacuum bag pressure began to erode after 140 seconds. It was also badly cracked (see fig. 17(a)). The material molded at 1000 psia (6890 kN/m^2) did not erode but combustion gas leakage caused termination after 55 seconds. The material was cracked (see fig. 17(b)), but not as badly as the lower pressure molding. The material molded at the higher pressure apparently withstood the thermal stresses better. These results illustrate the difficulty of making castable or trowelable materials to withstand the rocket engine environment. The higher pressure molding should be tested in a thinner piece - possibly as a throat insert - to reduce thermal stresses.

A carbon cloth - phenolic resin ablative material (FM5055A) began erosion after 91 seconds. The mode of failure was structural, probably caused by the carbon reinforcement being too weak to withstand the applied shear forces at the test temperature. Figure 18 shows the failure experienced, particularly the material chunking at the throat plane. The holes illustrate resin decomposition blow holes caused by the high heat flux.

A graphite cloth - phenolic resin ablative material (FM5064) was tested for 300 seconds and experienced no erosion. The firing was terminated by a timer since the design objective had been met. A section view of the nozzle is given in figure 19. It was concluded that graphite-phenolic ablatives are suitable for extended duration firings at 100-psia (689-kN/m^2) chamber pressure. Since the main objectives of the program had been met, it was decided to explore the effects of chamber pressure and O/F variations on graphite-phenolic ablatives.

Effect of chamber pressure on material performance. - The effect of chamber pressure on throat erosion was determined using the same graphite cloth - phenolic resin material (FM5064) and nozzle design described in the preceding section.

The change in throat radius is plotted in figure 20 as a function of run time for chamber pressures of 100, 150, and 200 psi (689, 1032, and 1378 kN/m^2). The negative throat area change noted on the curve at 100-psia (689-kN/m^2) chamber pressure was determined to be caused by deposition of alternate layers of carbon and pyrolytic graphite. The inside layer was pyrolytic graphite with its characteristic shiny hardness. We felt that deposits were formed because the nozzle wall presented the proper variations in temperature, pressure, and chemical species for the alternate deposition of pyrolytic graphite and carbon. Figure 21 is a post-test photograph of the nozzle showing the deposits at the throat. The deposits were concentrated over one-third of the throat circumference and had a maximum thickness of $1/8$ inch (0.316 cm). The uneven deposits were apparently due to uneven O/F distribution from the injector since they extend the length of the ablative section. The solution to the deposition problem would be (1) to assure even O/F distribution from the injector and (2) to run at an overall O/F high enough



C-67-4211

Figure 18. - Carbon-phenolic (FM5055A) after 173-second run. Chamber pressure, 100 psia (689 kN/m^2); FLOX-propane fuel; oxidant-to-fuel ratio, 4.5.



C-68-4125

Figure 19. - Graphite-phenolic (FM5064) after 300-second run. Chamber pressure, 100 psia (689 kN/m^2); FLOX-propane fuel; oxidant-to-fuel ratio, 4.5.

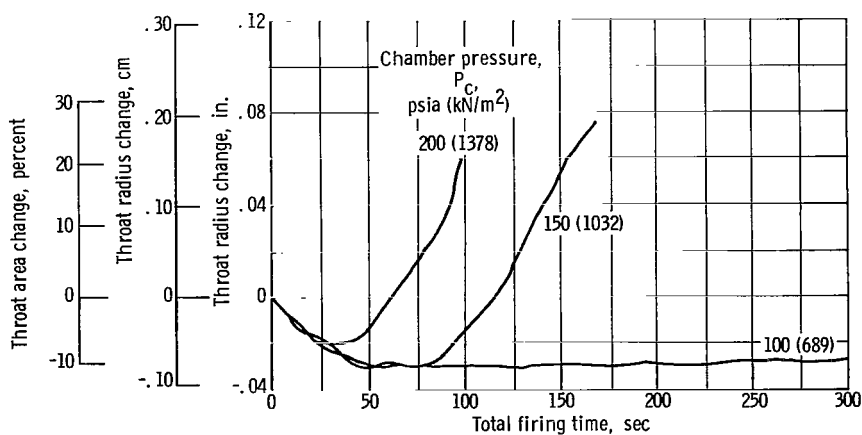


Figure 20. - Chamber pressure effect on ablative erosion of graphite-phenolic (FM5064, 60° centerline); throat diameter, 1.2 inches (3.05 cm); FLOX-propane fuel; oxidant-to-fuel ratio, 4.5; injector 6.

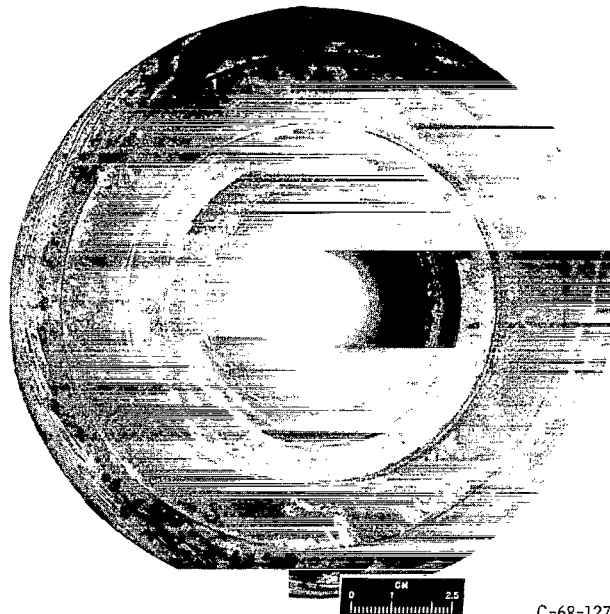
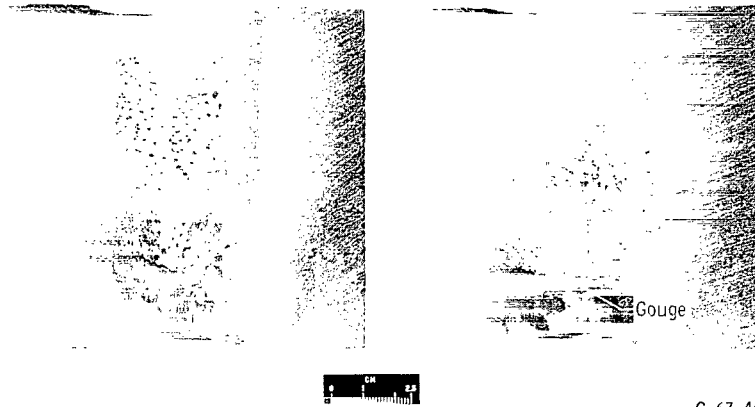


Figure 21. - Graphite-phenolic (FM5064, 60° centerline) after 300-second firing time. Chamber pressure, 100 psia (689 kN/m²); injector 6.

to prevent deposition but low enough to prevent oxidation. As shown in figure 20, depositions did occur for 150- and 200-psia (1032- and 1378-kN/m²) chamber pressures. Combined effects of higher temperature and higher shear forces gradually removed the deposits, however.

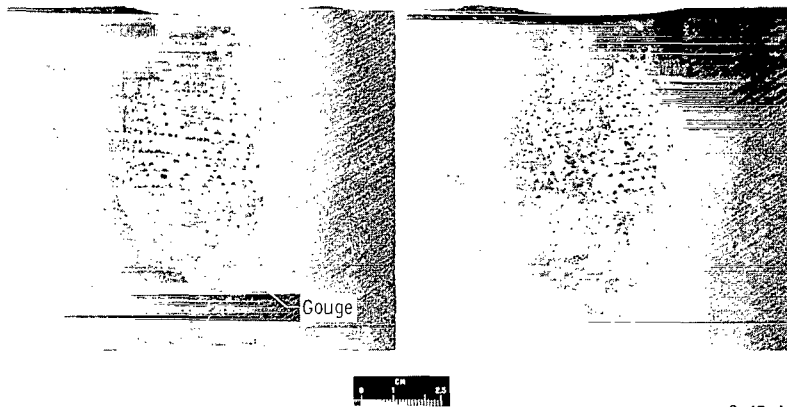
The nozzles tested at 150 and 200 psia (1032 and 1378 kN/m²) were allowed to erode until a steady-state rate had been established. The material chunking at the throat plane was similar to that of the carbon phenolic nozzle discussed earlier. The material loss was apparently due to the increased shear forces at the higher chamber pressure level, which exceeded the strength of the reinforcement at the operating temperature. The post-test photographs (fig. 22(a) for 150 psia (1032 kN/m²) and fig. 22(b) for 200 psia (1378 kN/m²)) illustrate the shear failure of the reinforcement-char combination. Graphite cloth - phenolic resin ablative material (FM5064) was satisfactory for long-duration firings at 100-psia (689-kN/m²) chamber pressure but not at 150-psia (1032-kN/m²) chamber pressure or above.

Effect of oxidant-to-fuel ratio on material performance. - A chamber pressure of 200 psia (1378 kN/m²) was chosen to evaluate the effect of oxidant-to-fuel ratio on ablative erosion since it provided significant erosion in a minimum of firing time. A graphite cloth - phenolic resin ablative material (FM5064) with the fabric oriented at 60° to the nozzle centerline was again used. Figure 23 shows the change in throat radius as a function of firing time at oxidant-to-fuel ratios of 3.4, 4.5, and 5.0.



C-67-4493

(a) Firing time, 170 seconds; chamber pressure, 150 psia (1032 kN/m²).



C-67-4494

(b) Firing time, 99 seconds; chamber pressure, 200 psia (1378 kN/m²).

Figure 22. - Shear failure of reinforcement-char combination. Material, graphite-phenolic (FM5064); FLOX-propane fuel; oxidant-to-fuel ratio, 4.5.

The erosion curves illustrate the difference in carbon deposition at the start of each separate O/F test. The longer run duration at an O/F of 3.5 was probably due to the increase in carbon available in the combustion gases and subsequent protection by deposition on the nozzle walls. The calculated experimental combustion gas temperature was 7270° R (4040 K) at both 4.5 and 5.0 O/F, which compares to a calculated experimental combustion gas temperature of 6740° R (3742 K) at an O/F of 3.5. The 530° R (294 K) difference in temperature was probably not sufficient to explain the erosion difference. Rather, the pyrolytic graphite deposition at the low O/F protected the underlying ablative from the stream shear and thermal effects. The reason for the erosion at the low O/F after 140 seconds was because of the nonuniformity of carbon deposition illustrated in figure 24(a).

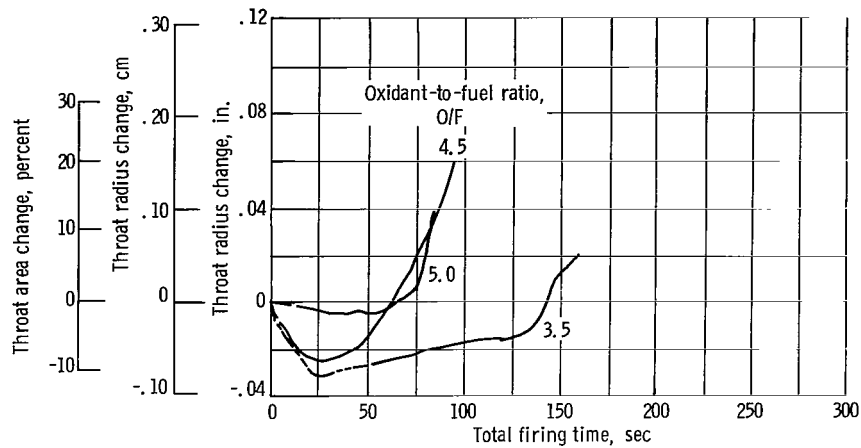
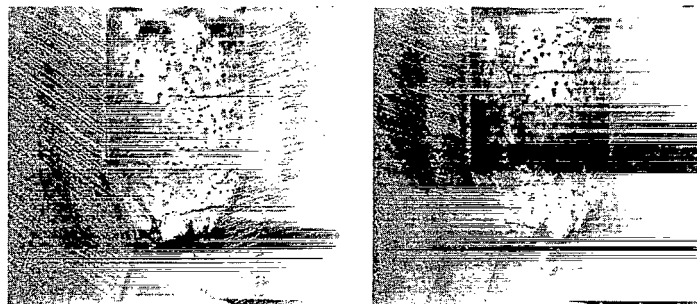


Figure 23. - Oxidant-to-fuel ratio effect on ablative erosion of graphite-phenolic (FM5064, 60° centerline); throat diameter, 1.2 inches (3.05 cm); FLOX-propane fuel; chamber pressure, 200 psia (1378 kN/m²); injector 6.



C-68-4371

(a) Oxidant-to-fuel ratio, 3.5; total firing time, 151 seconds.



C-68-4372

(b) Oxidant-to-fuel ratio, 5.0; total firing time, 82 seconds.

Figure 24. - Carbon deposition. Graphite-phenolic material (FM5064, 60° centerline); chamber pressure, 100 psia (689 kN/m²); FLOX-propane fuel.

These data illustrate the sensitivity of ablative erosion to O/F. For these experiments, the overall O/F was varied. Proper O/F for ablative compatibility can also be attained by O/F zoning of the injector.

Figure 24(a) illustrates the material after testing at an O/F of 3.5, and figure 24(b) illustrates the material after testing at an O/F of 5.0.

Throat insert testing. - Figure 25 is a plot of the erosion against firing time for an ATJ graphite throat insert at 200 psia (1378 kN/m^2) and an O/F of 3.5. The lower O/F was used to prevent failure by oxidation. The throat area decrease illustrates carbon deposition which could be attained by O/F zoning of the injector.

The insert firing was ended after 195 seconds because of a combustion gas leak. The ablative material including the silica-phenolic outer layer was completely charred by the firing. These nozzles were designed for 100-psia (689-kN/m^2) chamber pressure and 300 seconds operation. The design proved inadequate for 200-psia (1378-kN/m^2) chamber pressure and 300 seconds. A thicker ablative wall or use of more insulating ablative materials such as asbestos-phenolic or carbon-phenolic is required to prevent

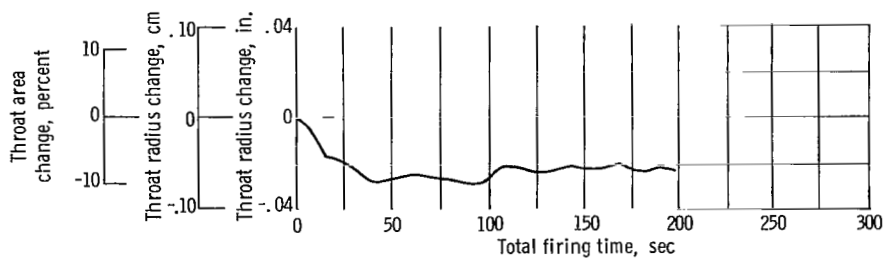
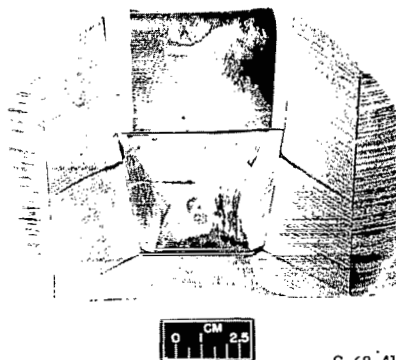


Figure 25. - Performance of ATJ graphite throat insert. Chamber pressure, 200 psia (1378 kN/m^2); throat diameter, 1.2 inches (3.05 cm); FLOX-propane fuel; oxidant-to-fuel ratio, 3.5.



C-68-4119

Figure 26. - ATJ graphite insert after 195-second firing time. Chamber pressure, 200 psia (1378 kN/m^2); FLOX-propane fuel; oxidant-to-fuel ratio, 3.5.

charthrough. Figure 26 illustrates the condition of the nozzle after testing. The graphite deposits were evident, as was a crack in the insert structure. Since a wide range of graphite materials are available, crack-free inserts could most likely be obtained to provide satisfactory engine operation for long-time duty cycles at chamber pressures of 200 psia (1378 kN/m^2) and higher.

Vacuum specific impulse. - A curve of experimental vacuum specific impulse for injector 6 (fig. 27) shows that performance is not sacrificed in shifting the mixture from an O/F of 4.5 to 3.5. In fact, results indicate operation at an O/F of 3.5 instead of an O/F of 4.5 would result in a specific impulse gain of 6 seconds, using a nozzle with an expansion area ratio of 2.0. There is some disadvantage in the lower O/F as a result of a reduction in the overall propellant density. However, the magnitude of this effect is strongly dependent on mission requirements, and some trade-off would be necessary.

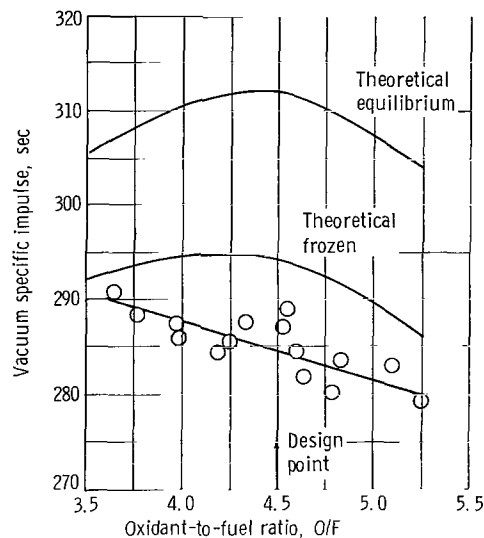


Figure 27. - Vacuum specific impulse of injector 6. Chamber pressure, 100 psia (689 kN/m^2); throat diameter, 1.2 inches (3.05 cm); FLOX-propane fuel; expansion area ratio, 2.0.

SUMMARY OF RESULTS

A program was conducted to design and test a rocket engine with a 1.2-inch (3.05-cm) throat diameter having a characteristic exhaust velocity efficiency of 95 percent or better, stable combustion, and a 300-second continuous firing capability.

The results of the program are as follows:

1. An oxidant-fuel-oxidant triplet injector with the elements mutually perpendicular was designed and tested. The ηC^* was 95.4 percent (97.5 percent corrected for heat

losses) at a chamber pressure of 100 psia (689 kN/m^2) and an O/F of 4.5. The ηC^* was 97.2 percent (99.3 percent corrected for heat losses) at a chamber pressure of 200 psia (1378 kN/m^2) and an O/F of 4.5. Combustion was stable over the entire range of operation.

2. At 100-psia (689-kN/m^2) chamber pressure, a characteristic length L^* of 33 inches (83.8 cm) for the combustion chamber was necessary to achieve a characteristic exhaust velocity efficiency ηC^* of 95 percent delivered (97.5 percent corrected for heat losses), and no significant increase in performance was measured with an L^* of 51 inches (129.5 cm).

3. Ablative materials containing graphite cloth reinforcement were superior in erosion resistance to ablatives using carbon or silica cloth as the reinforcement, and a 300-second continuous firing capability was demonstrated at 100-psia (689-kN/m^2) chamber pressure.

4. Carbon and/or graphite deposition on graphite phenolic from the propellant combustion gases decreased the throat area by 10 percent for 300-second firing duration at 100-psia (689-kN/m^2) chamber pressure and an oxidant-to-fuel ratio (O/F) of 4.5.

5. The rate of carbon-graphite deposition is apparently a function of the local O/F in conjunction with the effective wall surface temperature. Control of the local O/F can probably be accomplished by O/F zoning of the injector.

6. A graphite cloth - phenolic ablative nozzle provided erosion-free operation for only 60 seconds at a chamber pressure of 200 psia (1378 kN/m^2) and O/F of 4.5 and 5.0. Decreasing the O/F to 3.5 at 200-psia (1378-kN/m^2) chamber pressure extended the erosion-free firing time to 140 seconds.

7. At chamber pressures of 150 psia (1032 kN/m^2) and higher, a throat insert such as monolithic graphite is required to resist the local shear forces. A continuous run of 195 seconds was demonstrated at 200-psia (1378-kN/m^2) chamber pressure and an O/F of 3.5 with an ATJ graphite insert. Longer firing durations require redesign of the ablative envelope to prevent charthrough.

8. Operation of the oxidant-fuel-oxidant triplet injector at 100-psia (689-kN/m^2) chamber pressure and an O/F of 3.5, provided a delivered impulse gain of 6 seconds compared to operation at the theoretical maximum impulse O/F of 4.5.

Lewis Research Center,
National Aeronautics and Space Administration,
Cleveland, Ohio, March 28, 1969,
128-31-36-02-22.

APPENDIX - SYMBOLS

A_f	fuel injection area, ft^2 ; m^2
A_{ox}	oxidant injection area, ft^2 ; m^2
A_t	throat area, in.^2 ; cm^2
C_d	nozzle discharge coefficient (determined as in ref. 3), 0.985
D_e	rocket nozzle exit diameter, in.; cm
D_t	throat diameter, in.; cm
F	thrust, lbf; N
F_{vac}	vacuum thrust, $F + (P_o D_e^2 \pi / 4)$, lbf; N
g	gravitational constant, 32.174 ft/sec^2 ; 9.8 m/sec^2
I_{vac}	vacuum specific impulse, F_{vac}/W_p , sec
$I_{\text{vac, th, eq}}$	theoretical vacuum specific impulse determined by methods of ref. 6
L	length
L^*	characteristic chamber length, V_c/A_t , in.; cm
O/F	oxidant-fuel ratio, W_{ox}/W_f
P_c	chamber pressure measured at injector, psia; kN/m^2
$P_{c, \text{corr}}$	total pressure at rocket throat (determined as in ref. 3), $0.98 P_c$, psia; kN/m^2
P_o	ambient pressure surrounding engine, psia; kN/m^2
R_i	initial throat radius, in.; cm
R_t	throat radius at any time, $\sqrt{W_p \eta C_k^* C_{\text{th}}^* / \pi g P_{c, \text{corr}} C_d}$, in.; cm
ΔR_{eff}	effective throat radius change, $R_t - R_i$, in.; cm
V_c	chamber volume, in.^3 ; cm^3
v_f	fuel injection velocity, $W_f/\rho_f A_f$, ft/sec; m/sec
v_{ox}	oxidant injection velocity, $W_{\text{ox}}/\rho_{\text{ox}} A_{\text{ox}}$
W	weight flow, lb/sec; kg/sec
W_p	total propellant weight flow, lb/sec; kg/sec
ηC_{exp}^*	experimental characteristic exhaust velocity efficiency, $\eta I_{\text{sp}}/C_{F, \text{vac}}$
$\eta C_{F, \text{vac}}$	vacuum thrust coefficient efficiency (determined by methods of ref. 3), 0.962

ηC_K^* constant ηC^* efficiency, determined from calibration firings of a given injector

ηI_{sp} specific impulse efficiency, $I_{vac, exp}/I_{vac, th, eq}$

ρ density, lb/ft³; kg/m³

Subscripts:

c chamber

E engine

f fuel

ox oxidant

REFERENCES

1. Anon.: Investigation of Light Hydrocarbon Fuels with FLOX Mixtures as Liquid Rocket Propellants. PWA-FR-1443, Pratt and Whitney Aircraft (NASA CR-54445), Sept. 1, 1965.
2. Priem, Richard J.; and Heidmann, Marcus F.: Propellant Vaporization as a Design Criterion for Rocket-Engine Combustion Chambers. NASA TR R-67, 1960.
3. Shinn, Arthus M., Jr.: Experimental Evaluation of Six Ablative-Material Thrust Chambers as Components of Storable-Propellant Rocket Engines. NASA TN D-3945, 1967.
4. Burns, E. A.; Lubowitz, H. R.; Jones, J. F.; and Nordberg, R. C.: Investigation of Resin Systems for Improved Ablative Materials. TRW-4550-6007-R0000, TRW Systems (NASA CR-72022), July 25, 1966.
5. Elverum, G. W., Jr.; and Morey, T. F.: Criteria for Optimum Mixture-Ratio Distribution Using Several Types of Impinging-Stream Injector Elements. Memo 30-5, Jet Propulsion Lab., California Inst. Tech., Feb. 25, 1959.
6. Zeleznik, Frank J.; and Gordon, Sanford: A General IBM 704 or 7090 Computer Program for Computation of Chemical Equilibrium Compositions, Rocket Performance, and Chapman-Jouguet Detonations. NASA TN D-1454, 1962.



POSTAGE AND FEES PAID
NATIONAL AERONAUTICS AND
SPACE ADMINISTRATION

07U 001 53 51 3DS 69178 00903
AIR FORCE WEAPONS LABORATORY/AFWL/
KIRTLAND AIR FORCE BASE, NEW MEXICO 87117

ATTN: L. LUD. BOWMAN, ACTING CHIEF TECH. LIAISON

POSTMASTER: If Undeliverable (Section 151
Postal Manual) Do Not Return

"The aeronautical and space activities of the United States shall be conducted so as to contribute . . . to the expansion of human knowledge of phenomena in the atmosphere and space. The Administration shall provide for the widest practicable and appropriate dissemination of information concerning its activities and the results thereof."

—NATIONAL AERONAUTICS AND SPACE ACT OF 1958

NASA SCIENTIFIC AND TECHNICAL PUBLICATIONS

TECHNICAL REPORTS: Scientific and technical information considered important, complete, and a lasting contribution to existing knowledge.

TECHNICAL NOTES: Information less broad in scope but nevertheless of importance as a contribution to existing knowledge.

TECHNICAL MEMORANDUMS: Information receiving limited distribution because of preliminary data, security classification, or other reasons.

CONTRACTOR REPORTS: Scientific and technical information generated under a NASA contract or grant and considered an important contribution to existing knowledge.

TECHNICAL TRANSLATIONS: Information published in a foreign language considered to merit NASA distribution in English.

SPECIAL PUBLICATIONS: Information derived from or of value to NASA activities. Publications include conference proceedings, monographs, data compilations, handbooks, sourcebooks, and special bibliographies.

TECHNOLOGY UTILIZATION PUBLICATIONS: Information on technology used by NASA that may be of particular interest in commercial and other non-aerospace applications. Publications include Tech Briefs, Technology Utilization Reports and Notes, and Technology Surveys.

Details on the availability of these publications may be obtained from:

SCIENTIFIC AND TECHNICAL INFORMATION DIVISION
NATIONAL AERONAUTICS AND SPACE ADMINISTRATION
Washington, D.C. 20546